

THE REMOVAL OF ACID TEXTILE DYES BY ADSORPTION METHOD: OPTIMIZATION, KINETICS, ISOTHERM, AND THERMODYNAMICS

¹Mehmet TÜRKYILMAZ , ^{2,*}Farabi TEMEL 

¹ Konya Technical University, Engineering and Natural Sciences Faculty, Environmental Engineering Department, Konya, TÜRKİYE

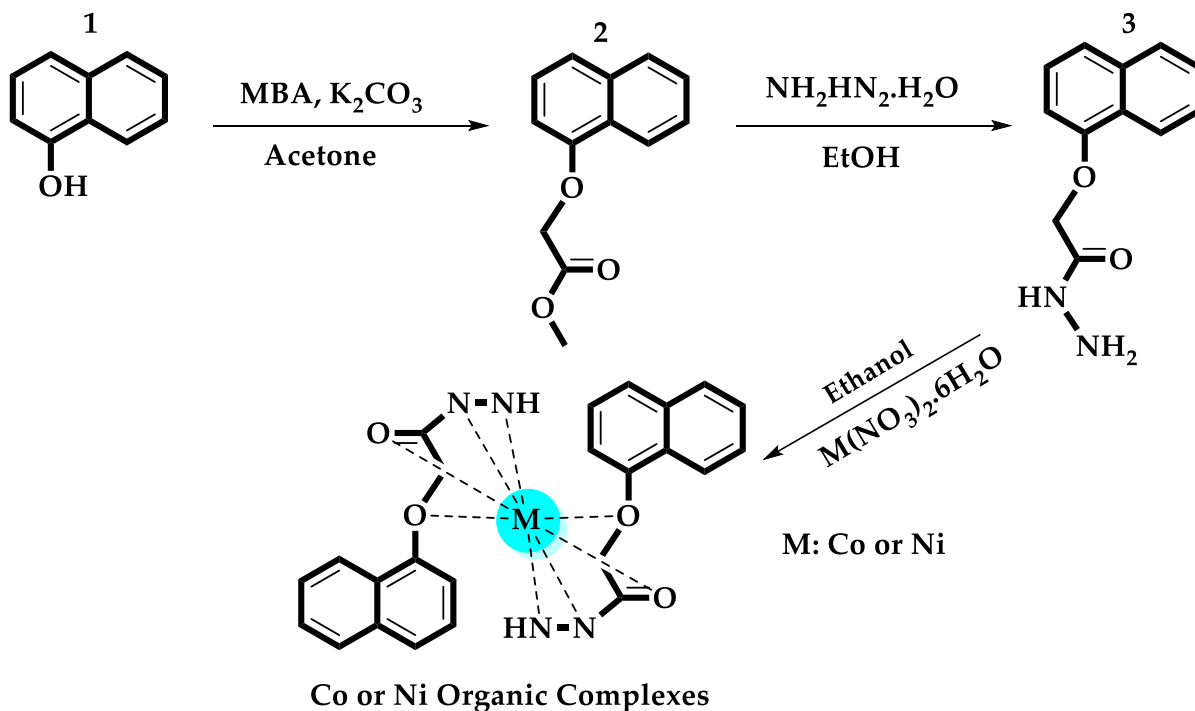
² Konya Technical University, Engineering and Natural Sciences Faculty, Chemical Engineering Department, Konya, TÜRKİYE

¹mturkyilmaz@ktun.edu.tr, ²ftemel@ktun.edu.tr

Highlights

- The Co or Ni/compound 3 complexes were successfully prepared and used as adsorbents.
- The adsorbent was tested with real samples, such as textile wastewater.
- Adsorption studies were analyzed based on thermodynamics, kinetics, and isotherms.
- High removal efficiencies and adsorbent capacities were achieved for acid dyes.

Graphical Abstract



Synthetic pathway of Co or Ni organic complexes

THE REMOVAL OF ACID TEXTILE DYES BY ADSORPTION METHOD: OPTIMIZATION, KINETICS, ISOTHERM, AND THERMODYNAMICS

¹Mehmet TÜRKYILMAZ , ^{2,*}Farabi TEMEL 

¹ Konya Technical University, Engineering and Natural Sciences Faculty, Environmental Engineering Department, Konya, TÜRKİYE

² Konya Technical University, Engineering and Natural Sciences Faculty, Chemical Engineering Department, Konya, TÜRKİYE

¹mturkyilmaz@ktun.edu.tr, ²ftemel@ktun.edu.tr

(Received: 25.06.2025; Accepted in Revised Form: 08.08.2025)

ABSTRACT: In this study, the removal of Acid Red 337 (AR 337) and Bemacid Red (BR) dyes from aqueous solutions by the synthesized Co or Ni 2-(naphthalen-1-yloxy) acetohydrazide adsorbents (Co or Ni/compound **3** complexes) was investigated. Therefore, 2-(naphthalen-1-yloxy) acetohydrazide was synthesized from 1-naphthol, and the complexation of this compound with Cobalt or Nickel metal was carried out to obtain an adsorbent. The structures of the obtained compounds were characterized by ¹H NMR and FT-IR. In further experiments, the batch method was conducted and evaluated based on contact time (1-60 min), pH (3-12), the dosage of Co or Ni organic complexes (0.02-0.2 g/L), and initial dye concentration (15-100 mg/L) regarding removal efficiency. The optimum conditions from the experimental data were obtained as 50 mg/L BR-100 mg/L AR 337 initial concentration, pH 6.7, 25-40 min. contact time, and 0.1 g adsorbent dosage for BR and AR 337 dyes, respectively. The maximum adsorption capacity obtained under optimum conditions was calculated as 461.14 and 861.8 mg/g for BR and AR 337, respectively, for a contact time of 40 min. Additionally, the Langmuir, Freundlich, Dubinin-Radushkevich, and Temkin isotherm models, along with the Pseudo-first-order, Pseudo-second-order, Weber-Morris, and Evolvich kinetic models, were applied to the experimentally obtained results under optimal conditions, and the model constants were calculated. When R² values were evaluated in terms of adsorption kinetics, it was seen that the pseudo-second-order kinetic model was a more compatible model for both dyes. Additionally, high correlation coefficients for BR and AR 337 were obtained in Temkin and Langmuir adsorption isotherm models, respectively. Thermodynamic analyses: It was found that the enthalpy change of AR 337 dye ($\Delta H^\circ < 0$) was negative and, therefore, exothermic, while the enthalpy change for BR ($\Delta H^\circ > 0$) was positive and, therefore, endothermic. The fact that the standard free energy change ($|\Delta G^\circ| > 20$ kJ/mol) values were negative for both dyes indicates that the adsorption was physical and spontaneous. As a result, the proposed Co or Ni organic complexes were found to be promising in dye removal.

Keywords: Acid Dyes, Adsorption Mechanism, Co or Ni/Organic Complexes

1. INTRODUCTION

Water is one of the basic requirements that all living things need. However, due to the rapid developments in industrialization, drought, and the growth of the world population, the protection of clean water resources is becoming an important issue today [1]. Despite this, water consumption is quite high in many processes such as production, washing, evaporation, drying, and energy production [2]. The textile industry, where synthetic dyes are used intensively, is one of the largest industrial branches that cause water pollution. Up to 450 m³/ton of water may be required during the textile production process, and approximately 80% of this water turns into wastewater that needs to be treated before being discharged into the receiving environment [3]. This wastewater contains 20-40% dyes due to the fact that the dyes used in the dyeing process are not fixed to the product [4]. Dye pollution in wastewater from dye industries raises concerns about toxicology. Under anaerobic conditions, the decomposition of some

*Corresponding Author: Farabi TEMEL, ftemel@ktun.edu.tr

types of dyes poses a risk to all living organisms in the trophic chain, including human health, as it leads to the formation of intermediate compounds such as carcinogenic aromatic amines [5]. Therefore, the treatment of textile industry wastewater is an important environmental requirement due to the potential pollution that may occur in surface waters and groundwater.

Dyes are generally difficult to purify in traditional purification processes due to their complex aromatic structures, low degradability, resistance to degradation in sunlight, and highly effective assimilation [6]. For the treatment of a large amount of wastewater, physical-physicochemical methods such as coagulation-flocculation [7], ion exchange [8], adsorption [9] and membrane filtration [10], chemical methods such as chemical oxidation and ozonation [11, 12], biological methods such as aerobic or anaerobic digestion [13] and electrochemical methods [14] are applied. Adsorption, which is a physical method, has advantages over other methods due to its features, such as having a reasonable initial cost and simple design, being relatively easy to maintain and operate, insensitive to pollutant toxicity, efficient and environmentally friendly with less energy consumption [15]. To date, a wide range of low-cost adsorbents, including activated carbons, zeolites, clays, silica beads, agricultural wastes, biomass, industrial by-products, and polymeric resins, have been utilized for wastewater treatment, particularly for dye removal [16-19]. Known adsorbents generally have low adsorption capacity due to limited surface area or active sites, and their selectivity is also limited [20]. These days, developing new adsorbents with superior properties, such as high and rapid adsorption capacity and stability, for use in removing pollution from wastewater is a significant area of research. The use of organic compounds in adsorption processes is quite challenging due to their dispersibility in water and hydrophobic properties. Therefore, the use of potential complexes with metals in adsorption studies is quite common to impart hydrophilic properties to organic compounds and enhance their interaction with contaminants in water. Furthermore, the idea that the use of transition metals in adsorbents, due to differences in their electronic properties, may increase their affinity for contaminants in aqueous environments, supports the use of complexes of metals with organic ligands as adsorbents [21]. For this purpose, the aim was to improve the adsorption properties by adding different percentages of Ni and Co metal ions to 2-(naphthalen-1-yloxy) acetohydrazide (compound **3**). Since the adsorption process is particularly effective for acid dyes, acid dyes are widely used due to their high water solubility, and they are considered to be the most environmentally problematic dyes because they are not affected by conventional treatment systems, the efficiencies of the adsorbents (Co or Ni organic complexes) were tested on BR and AR 337 acid dyes as reference pollutants. For this purpose, the effects of pH, adsorbent dosage, pollutant concentration, and contact time on dye removal were studied and optimized. To explain the adsorption mechanism, adsorption results were assessed in terms of isotherm, kinetic, and thermodynamic studies, with the findings presented below.

2. MATERIAL AND METHODS

2.1. Reagents and instrumentation

All reagents and solvents were purchased as analytical grade from Merck or Aldrich. Therefore, they were used without any pre-purification process. The reactions were controlled by analytical thin layer chromatography (TLC) using silica gel plates (SiO₂, Merck F₂₅₄). In addition, ¹H NMR and FT-IR spectra for the characterization of the materials were taken with a Varian 400 MHz NMR and a Perkin Elmer 100 FT-IR spectrometer, respectively. Also, the dye materials used were purchased from DyStar. AR 337 and BR dye solutions, ranging from 20 to 500 mg/L, were prepared with deionized water (Millipore Milli-Q Plus).

2.2. Synthesis Pathway of Metal Organic Complexes

The synthesis pathway of Co or Ni / 2-(naphthalen-1-yloxy) acetohydrazide complex (Co or Ni organic complexes) was illustrated in Fig. 1. First, a mixture of 1 g 1-naphthol (**1**) and 1.11 g methyl

bromoacetate (MBA) in 50 mL acetone in the presence of anhydrous 0.575 g K_2CO_3 was refluxed for 24 h. After completion, the solvent was removed under vacuum, and the remaining solid was extracted using dichloromethane. Then, the organic phase was separated and dried with $MgSO_4$. The solvent was evaporated, and solid methyl 2-(naphthalen-1-yloxy)acetate (**2**) was obtained in 95% yield [22]. In the next step, 2-(naphthalen-1-yloxy) acetohydrazide (**3**) was synthesized from 1 g of methyl 2-(naphthalene-1-aryloxy) acetate (**2**) and 0.695 g of a hydrazine hydrate mixture in ethanol over 24 hours. After completion, the solvent was removed under vacuum, and the remaining solid was extracted using dichloromethane. Then, the organic phase was separated and dried with $MgSO_4$. The solvent was evaporated, and solid 2-(naphthalen-1-yloxy)acetohydrazide (**3**) was obtained in 85 % yield [23]. 1H NMR (400 MHz $CDCl_3$) δ 8.18-8.24 (b, 1H), 7.83-7.90 (m, 2H), 7.51-7.58 (m, 3H), 7.37-7.42 (t, 1H), 6.79-6.83 (d, 1H), 4.77-4.80 (s, 2H), 3.75-4.15 (b, 2H).

Finally, A mixture of 1g 2-(naphthalen-1-yloxy) acetohydrazide (**3**) and 0,726 g $Co(NO_3)_2 \cdot 6H_2O$ or $Ni(NO_3)_2 \cdot 6H_2O$ was refluxed in 50 mL ethanol for 24 h. After completion, the reaction medium was filtered and washed with ethanol to remove impurities. Then, it was dried in an oven at 100 °C for 1 day. The solid Co or Ni organic complex was obtained [24].

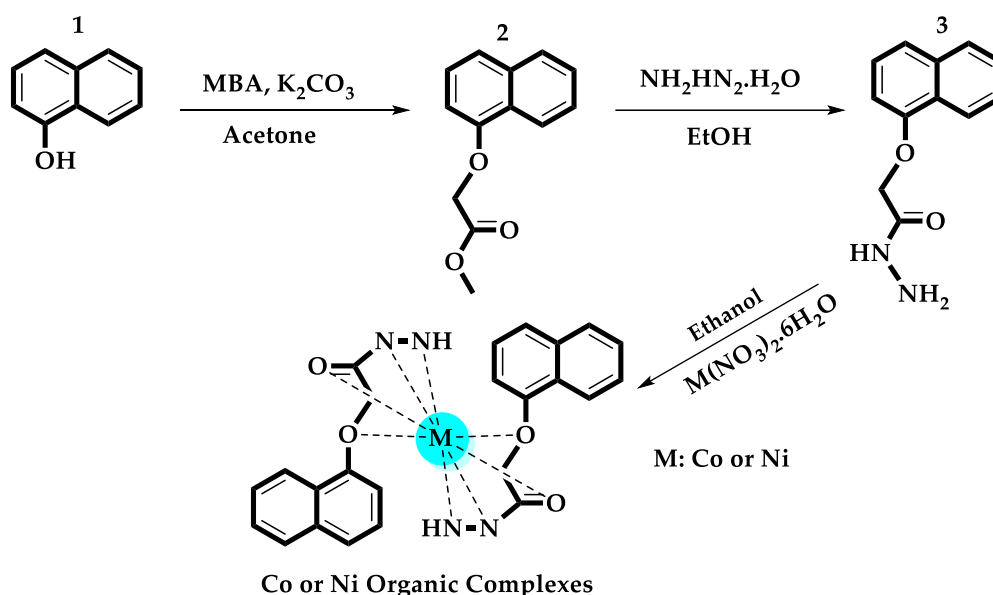


Figure 1. Synthetic pathway of Co or Ni organic complexes.

2.3. Adsorption Experiments

In this study, the effectiveness of the adsorbent in the removal of BR and AR 337 dyes from aqueous solutions was investigated with the pure compound **3** and Co or Ni organic complex forms. First, experiments were conducted at the original sample pH, 25 mg/L BR dye concentration, 0.1 g/L adsorbent dosage, and 30 min contact time to determine the highest removal efficiency among the produced adsorbents. After determining the effective adsorbent material, optimization of the adsorbent dosage (0.02-0.2 g/L), pH (3-12), contact time (1-60 min), and initial dye concentration (15-100 mg/L) was performed for BR and AR 337. After adsorption, the sample was centrifuged at 3000 rpm for 3 minutes to separate the adsorbent from the solution and make it ready for analysis. As a result of the batch experiments, the centrifuged samples were analyzed with a Shimadzu UV-1700 brand spectrophotometer (BR (λ_{max} = 524 nm) and AR 337 (λ_{max} = 500 nm)). The initial pH of each solution was adjusted to the required value with concentrated and diluted HCl and NaOH solutions before mixing the adsorbent into the solution. The removal efficiency and adsorption capacity (amount of dye adsorbed per weight of adsorbent) at a given time were calculated using the following equations.

$$\% \text{ dye removal} = ((C_o - C_e) / C_o) \times 100 \quad (1)$$

$$\% \text{ dye removal capacity} = ((C_o - C_e) / m) \times V \quad (2)$$

Where C_o and C_e denote the initial and equilibrium dye concentrations in the medium (mg/L), respectively, m and V represent the mass of the adsorbent (g) and the solution volume (L), respectively.

2.4. Adsorption Kinetics and Isotherm Models

To investigate the adsorption behavior between the adsorbent and BR and AR 337 dyes, the Langmuir, Freundlich, Dubinin-Radushkevich (D-R), and Temkin isotherm models, along with the pseudo-first order, pseudo-second order, intraparticle diffusion, and Evolvich kinetic models, were examined to describe the results of discrete experiments under optimal experimental conditions. The agreement between the predictions produced by the models and the experimental results was explained by the coefficient of determination (R^2).

According to the pseudo-first-order reaction model (Lagergren Equation) approach, the efficiency of physical adsorption and the number of adsorption points available for adsorption are directly proportional to the number of unused points (Equation 3) [25]. The pseudo-second order reaction model (Ho-McKay) assumes that chemisorption is dominant in the adsorption process due to electron exchange between the adsorbate and the adsorbent (Equation 4) [26]. The pseudo-second-order rate equation indicates that the rate does not depend on the adsorbate concentration but is influenced by the solid phase adsorption capacity and time. The Elovich model describes the chemisorption occurring on adsorbent materials with heterogeneous structures (Equation 5) [27]. The intraparticle diffusion model (Weber Morris Equation) describes the transfer of adsorbate to the adsorbent particles during the adsorption process (film diffusion, intraparticle diffusion, and adsorption) (Equation 6) [28].

$$\ln(q_e - q_t) = \ln q_e - k_1 t \quad (3)$$

$$t/q_t = 1/k_2 q_e + t/q_e \quad (4)$$

$$q_t = (1/\beta)(\ln \alpha \beta) + (1/\beta) \ln t \quad (5)$$

$$q_t = k_{id} \sqrt{t} + C \quad (6)$$

Here, t represents the contact time (min), α and β refer to the chemisorption rate (mg/g min) and a coefficient associated with surface coverage and activation energy for chemisorption (g/mg), respectively. k_{id} and C denote the rate constant (mg/g h^{1/2}) and a coefficient (mg/g) connected to the boundary layer size, respectively. q_e is the equilibrium adsorption capacity of the adsorbents (mg/g), k_1 is the Lagergren rate coefficient (1/min), and k_2 is the adsorption rate constant of the model (g/mg min).

The Langmuir model emphasizes that the adsorption process occurs uniformly and in a single layer (Equations 7-8) [29]. The Freundlich model posits that the adsorption process takes place heterogeneously and in multiple layers (Equation 9) [30]. The Tempkin model states that the adsorption process occurs uniformly and that the heat of molecular adsorption decreases linearly (Equation 10). [31]. The Dubinin-Radushkevich model is a general isotherm model used to test the nature of adsorption, based on the theory of potential change on a heterogeneous surface (Equations 11-13) [32].

$$C_e/q_e = (1/q_m K_L) + C_e/q_m \quad (7)$$

$$R_L = 1/(1 + K_L C_o) \quad (8)$$

$$\ln q_e = \ln K_F + (1/n) \ln C_e \quad (9)$$

$$q_e = (RT/b) \ln K_T + (RT/b) \ln C_e \quad (10)$$

$$\ln q_e = \ln q_m - K_{DR} \varepsilon^2 \quad (11)$$

$$\varepsilon = RT \ln [1 + 1/C_e] \quad (12)$$

$$E = 1/\sqrt{2} K_{DR} \quad (13)$$

Here, q_e represents the amount of adsorbate adsorbed per unit mass of adsorbent at equilibrium (mg/g). K_L refers to the affinity constant (L/mg). C_e and C_o indicate the equilibrium concentration (mg/L) and the inlet concentration (mg/L) of adsorbate, respectively. q_m refers to the maximum adsorption amount of adsorbate (mg/g). R_L indicates the dimensionless separation factor, while K_F and n correspond to constants related to adsorbent capacity (mg/g) and the degree of heterogeneity (L/g), respectively. R refers to the ideal gas constant (8.3145 J/mol K), T is the temperature (K) of the adsorption medium, b is a constant associated with the heat of adsorption (J/mol), K_T is the equilibrium binding constant associated with the binding energy, and K_{DR} refers to the isotherm constant associated with the adsorption energy. β indicates a constant based on the adsorption energy (mol²/kJ²), while ϵ and E correspond to the Polanyi potential and the average adsorption energy (kJ/mol), respectively.

2.5. Thermodynamic Analyses

Thermodynamic analyses were performed at four different temperatures: 20, 30, 40, and 50°C. The following equations were used to calculate thermodynamic parameters, including standard free energy change (ΔG°), enthalpy change (ΔH°), and entropy change (ΔS°) [33].

$$K_D = q_e/C_e \quad (14)$$

Here, K_D (partition coefficient) indicates the affinity of the adsorbent surface. Gibbs free energy is found using Equation 15 and is presented in Table 3.

$$\Delta G^\circ = -RT \ln K_D \quad (15)$$

ΔH° and ΔS° values were found using Equation 16 (Van't Hoff equation).

$$\ln K_D = (\Delta S^\circ/R) - (\Delta H^\circ/RT) \quad (16)$$

Here, R (8.314 J/mol/K) is the gas constant, and T (K) is the absolute temperature [34].

3. RESULTS AND DISCUSSION

3.1. Preparation and characterization of Metal Organic Complexes

In this work, Co or Ni organic complexes were prepared by the immobilization of Co(II) or Ni(II) as a metal ion on compound **3** (Fig. 1) to investigate the removal of acid textile dyes by the adsorption method. For this purpose, the 2-(naphthalen-1-yloxy)acetohydrazide (**3**), its proposed precursor methyl 2-(naphthalen-1-yloxy)acetate (**2**), and Co and Ni organic complexes were successfully prepared according to previously published procedures [22-24].

The proposed precursor 2-(naphthalen-1-yloxy) acetohydrazide (**3**) was characterized with ¹H NMR (Fig. 2). In Fig. 2, the structure of **3** was confirmed by the appearance of -NH protons at δ 8.18-8.24. Also, NH₂ and CH₂ protons were observed at δ 3.75-4.15 and 4.77-4.80, respectively. The formation of Co and Ni organic complexes was confirmed by the FT-IR spectra given in Fig. 3. In Fig. 3, the broad bands at 3224, 3292, and 3222 cm⁻¹ indicate that the -NH stretching vibration of hydrazine groups in Co or Ni organic complexes. Also, CH stretching vibrations on naphthol groups were observed at 3050, 3033, and 3054 cm⁻¹. The carbonyl group (C=O) asymmetric stretching bands were observed at 1656, 1658, and 1654 cm⁻¹, respectively. NH bending vibrations were observed at 1594, 1579, and 1596 cm⁻¹, respectively. The bands at 569, 559, and 569 cm⁻¹ indicate that the Co/Ni-O interactions, while the bands at 420, 408, and 418 cm⁻¹ indicate that the Co/Ni-N interactions for Co or Ni organic complexes [35, 36].

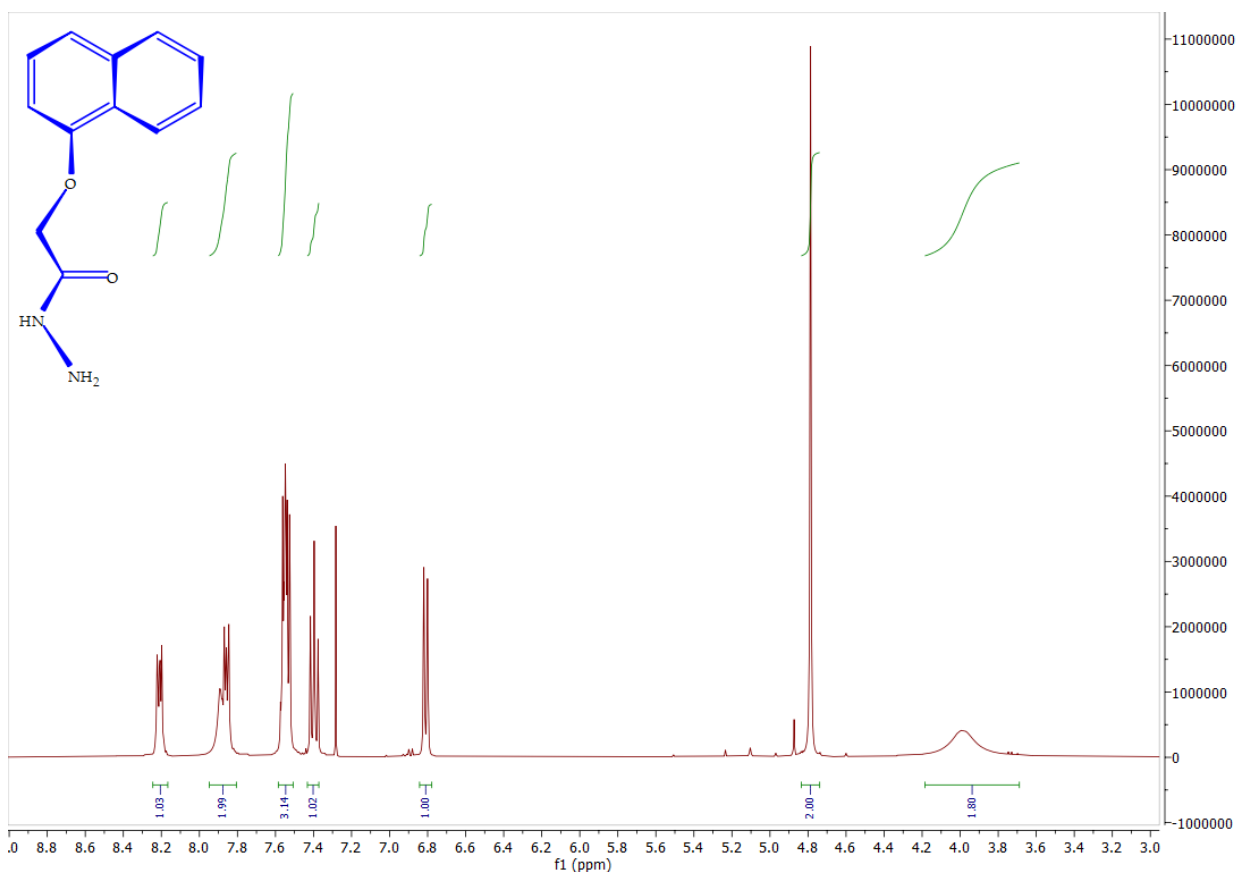


Figure 2. ¹H-NMR spectra of 2-(naphthalen-1-yloxy) acetohydrazide (3).

3.2. Comparison of Materials

The activities of Co or Ni organic complexes, consisting of a mixture of compound **3** and nickel-cobalt elements at different ratios, synthesized for use in adsorption experiments, were investigated.

For this purpose, the removal values obtained at the end of the 30-minute contact time using 0.1 g/L adsorbent material at the original sample pH (6.7) and 25 mg/L BR dye concentration are given in Fig. 4. When the figure is examined, it is seen that pure compound **3** has no adsorption activity, and the adsorption rate increases with the addition of Co or Ni elements to the synthesis. In addition, it is seen that the adsorption efficiency increases with the increase in the percentage of Co in the synthesized adsorbent, and the highest efficiency value is reached with the Co/compound **3** complex synthesized with 100% Co. In this case, the removal increased tremendously and reached 92.06%. By increasing the Co ratio from 25% to 100%, the removal increased by approximately 55%, which showed the effectiveness of the Co ratio on the adsorption process. However, while the presence of Ni and Co elements together had a positive effect compared to compound **3**, it had a negative effect compared to the synthesis made with only Co. Therefore, the optimization experiments were continued with 100% Co/compound **3** organic complex.

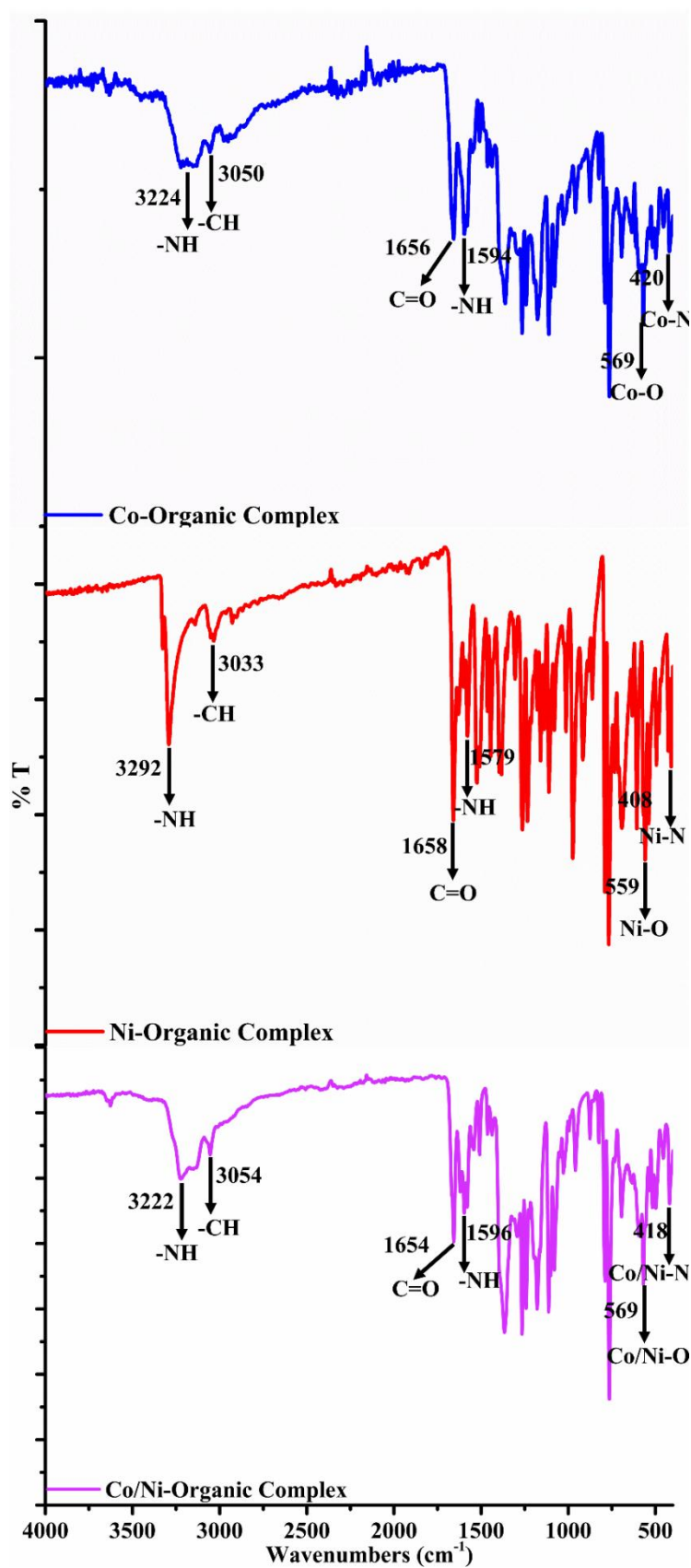


Figure 3. FTIR spectra of Co or Ni organic complexes.

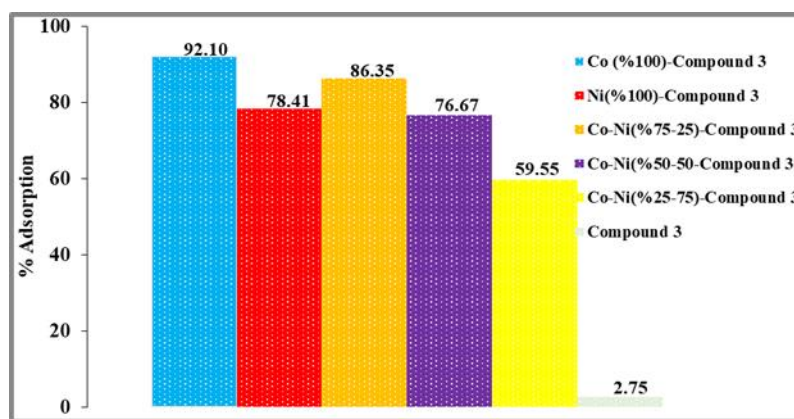


Figure 4. BR removal efficiency of synthesized adsorbents.

3.3. Effect of pH

Since pH affects the surface charge and active sites of the adsorbent, it is one of the most important parameters in the adsorption of organic dyes. The effects of various pH values (3-12) on removal were examined at an initial dye concentration of 50 mg/L, an adsorbent amount of 0.06 g/L, and a contact time of 30 minutes; the results are shown in Fig. 5. The original pH values of the samples were found to be optimum for both dyes. While 83.12% and 73.85% removal values were obtained for BR and AR 337 dyes, respectively, the highest capacity was reached at these pH values, 415.6 mg/g and 369.25 mg/g, respectively. According to the results, it is positive for the elimination of BR and AR 337 dyes in a weakly acidic environment. It indicates that pH significantly influences the behavior of the two dyes in solution. High acidic and basic conditions have a very negative effect on efficiency. With the increase of pH, the acidic active group (carboxylic, hydroxyl, and others) of the adsorbents is separated, and the surface of the adsorbent becomes negatively charged. Thus, the adsorption of cations is positively affected [37].

Douara, et al. [38] reported that the best retention rate by the biosorbent was obtained at pH 5.12 for BR with an adsorption capacity of 32.9 mg/g. They explained this phenomenon by the existence of a strong electrostatic attraction between the surface of the positively charged adsorbent and the anionic acid dye at a weakly acidic pH value. As the solution pH increases, the number of negatively charged sites will increase, while the number of positively charged sites will decrease. It was also stated that the low adsorption of the acid dye at alkaline pH is due to the presence of excess hydroxyl ions competing with the anions of the acid dye for adsorption sites, as in biomass (*Atriplex Halimus*). In their BR adsorption studies with Hranfa's marl, Maimoun, et al. [39] observed maximum dye adsorption at pH = 6. Yıldız [40] stated in his study that high q_e values were achieved at natural pH (without pH correction - pH: 7.3) for Acid Red 114 adsorption with $\text{Fe}_3\text{O}_4/\text{CFA}$ MNC. This was explained by the low solubility of $\text{Fe}_3\text{O}_4/\text{CFA}$ MNC at neutral pH.

3.4. Adsorbent Dosage Effect

When using an adsorbent, it is very important to determine the amount of adsorbent to be applied, not only from an economic point of view, but also from a technical performance point of view. The increase in adsorbent dosage increases the number of possible adsorption sites. Thus, the removal efficiency of the adsorbate increases. The basis of adsorbent dosage studies is to determine the use of the least possible adsorbent [37]. The effects of different adsorbent amounts (0.02-0.2 g/L) on removal were investigated at 50 mg/L initial dye concentration, original sample pH, 30 min contact time, and the results are shown in Figure 6. The increase in the adsorption amount had a similar effect for both dyes and increased efficiency up to the saturation point. For BR, the most effective removal with 91.18% was achieved with 0.1 g/L adsorbent amount. After this value, there was a slight decrease in efficiency with

increasing amount. When the values obtained for AR 337 were examined, 79.92% efficiency was achieved with 0.1 g/L of adsorbent amount. When the adsorbent amount was doubled, only 0.84 units of increase occurred in efficiency, and an 80.76% value was obtained. Since the increase in efficiency was negligible compared to the increase in adsorbent amount, the optimum adsorbent amount was accepted as 0.1 g/L.

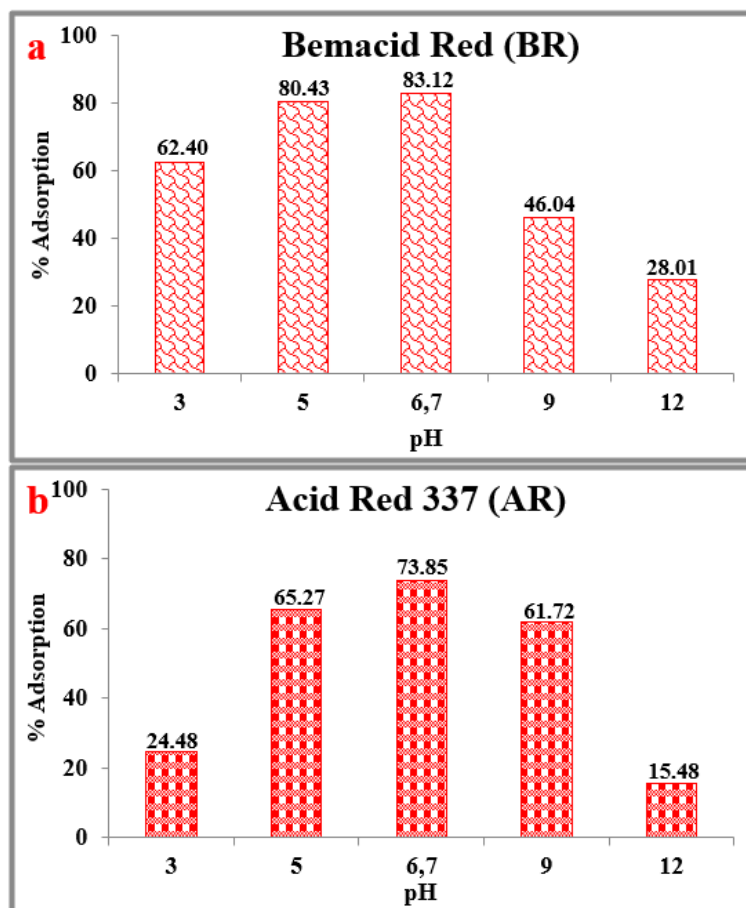


Figure 5. Effect of pH on the adsorption process of **a)** bemacid red (BR), and **b)** Acid red 337.

As the adsorbent amount increased, the dye removal rate increased due to the increased active surface area. The possible reason for the increase in the removal percentage with the increased adsorbent amount is that the surface area and the number of empty active sites increase with the increase in the adsorbent amount [41]. In a study using activated carbon derived from date seeds, it was reported that the removal efficiency of BR dye increased by approximately 4-fold when the adsorbent dosage was increased by 6-fold [42].

However, it has been stated that the increase in unsaturated active surface area can cause a significant decrease in adsorption capacity [43]. This situation occurs due to the unnecessary increase in the available surface area to hold the same amount of adsorbate on the adsorbent surface. In this study, the maximum capacity for BR dye reached 693.75 mg/g at an adsorbent dosage of 0.06 g/L, while capacity decreased with increasing dosage, ultimately decreasing to 206.5 mg/g. For AR 337, the highest capacity of 866.81 mg/g was achieved at an adsorbent dosage of 0.04 g/L, with the capacity decreasing as the dosage increased, eventually decreasing to 201.9 mg/g. Raca, et al. [44] found that the dye removal efficiency increased from 43.3% to 97.1% when the adsorbent amount was increased from 0.25 g to 4 g in BR adsorption on coal fly ash. Additionally, the lowest and highest adsorption capacities were determined at 1.2 mg BR/g ash and 8.4 mg BR/g ash for adsorbent masses of 4 g and 0.25 g, respectively. Feddane, et al. [45] reported that a removal efficiency of 65% (maximum) of BR textile dye was achieved

using 0.1 g of *Casuarina equisetifolia* needles. However, they noted that increasing the adsorbent dosage to reach maximum removal caused the adsorption capacity to decrease, eventually reaching a minimum value of 3.23 mg/g.

The presence of a larger amount of adsorbent in the adsorption medium causes the adsorption sites on the adsorbent surfaces to overlap and prevents efficient use of the surface area. In this case, the surface area of the adsorbent to which the adsorbate will adsorb decreases, which makes it difficult for the dye molecules to diffuse to the active areas where they will interact; thus, a decrease in efficiency is observed. Buntić, et al. [37] reported that the adsorption capacity decreases because most of the reactive sites for adsorption remain empty. The same situation was observed for AR 337, as reported in the studies by Özer, et al. [46] and Slatni, et al. [47].

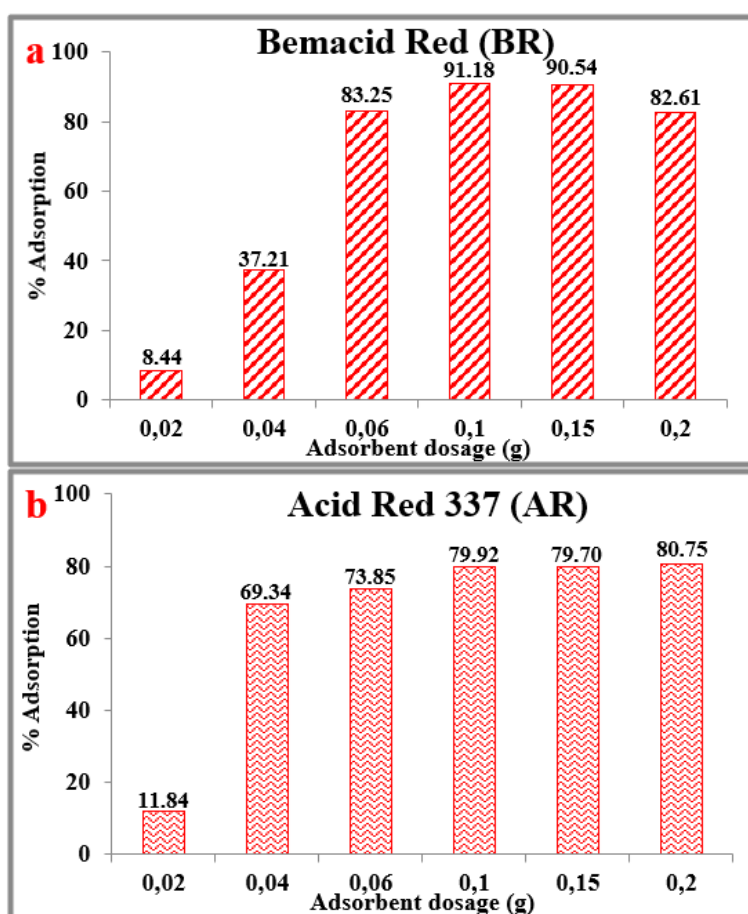


Figure 6. Effect of adsorbent dosage on removal of **a)** bemacid red (BR), and **b)** Acid red 337.

3.5. Effect of Dye Concentration

The initial concentration of the pollutant has a significant effect on the adsorption capacity of the adsorbent. In order to investigate its effect, different initial dye concentrations (15-150 mg/L) were examined at 0.1 g/L adsorbent amount, original sample pH, 30 min contact time, and the results are shown in Figure 7. As can be seen from the figure, there are different adsorption mechanisms for dyes. In the experiments conducted with BR dye, over 90% efficiency was obtained up to 50 mg/L concentration; after this value, the increase in pollutant concentration caused a serious decrease in efficiency. Since the level of pollutants remaining in the sample after the adsorption process at low dye concentrations falls below the device's measurement range, minor differences in the results can be disregarded. In this case, it can be assumed that the specified adsorbent amount for BR dye provides effective removal values up to 50 mg/L dye concentration. This is based on the fact that high dye

concentrations cause a high driving force that positively affects mass transfer. Although the adsorption capacity reached at 50 mg/L dye concentration was found to be 456 mg/g, it increased to 770 mg/g with the increase of dye concentration. The probable reason for this situation is thought to be the increase in the interactions between the dye and the adsorbent with the increase of the initial dye concentration [48] and the formation of a high driving force for mass transfer [49]. On the other hand, it can be observed that the removal efficiency is higher at lower dye concentrations. It is seen from the figure that as the initial concentration of the dye increases, the adsorption efficiency decreases due to the saturation of the existing adsorption sites on the adsorbent surface. In similar results obtained by Boudia, et al. [42], it was reported that the adsorption capacity of BR dye increased with increasing initial dye concentration in the solution.

Initial dye concentration plays a key role in providing the necessary driving force on the mass transfer resistance for the adsorption of a contaminant in aqueous solution onto a solid surface. Thus, in the experiments conducted with AR 337 dye, the efficiency increased with increasing dye concentration and reached 84.3% at a concentration of 100 mg/L. At this value, 843 mg/g adsorption capacity was reached, and with increasing concentration, the capacity increased up to 1237.5 mg/g, while the efficiency values decreased slightly, but generally reached equilibrium and did not change. This situation arises from the number of empty active sites on the surface for a given quantity of adsorbent, causing the dye adsorption to be inadequate as concentration increases [50]. The same phenomenon has been reported by other authors using different dyes [51, 52].

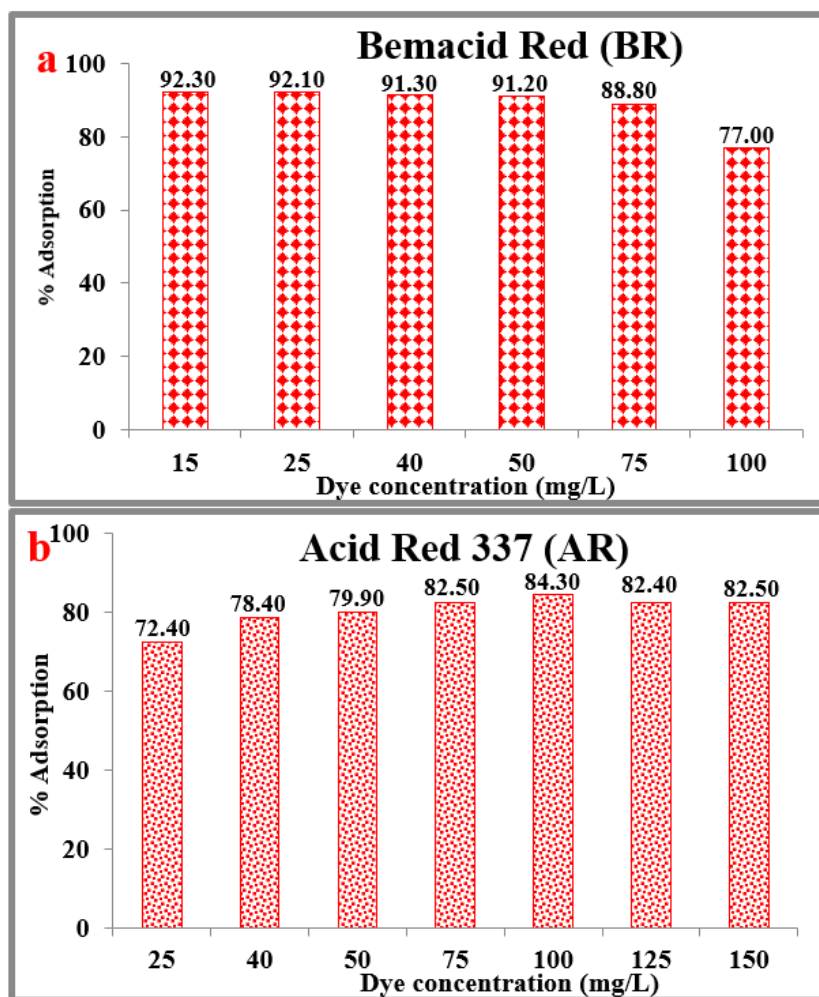


Figure 7. Effect of dye concentration on the adsorption process of **a)** bemacid red (BR), and **b)** Acid red 337.

3.6. Experiments with Real Textile Wastewater Sample

A wastewater sample resulting from dyeing was obtained from a textile workshop operating in Turkey for the dyeing of polyamide textile products. The dye recipe applied in the facility was created by mixing BR (CAS EINECS: 276-115-7, $M = 583.0$ g/mol), BB (CAS EINECS: 267-224-0, $M = 593.63$ g/mol) and AB 220 (CAS EINECS: 152287-07-5, $M = 1705.8$) acid dyes with citric acid and tanalev AFP chemicals in certain proportions. The effectiveness of the 100% Co/compound **3** complex in removing textile wastewater samples was examined by changing its concentration (0.4, 0.8, 1.2, and 1.6 g/L), and the results are given in Figure 8. The studies were conducted without changing the original wastewater pH.

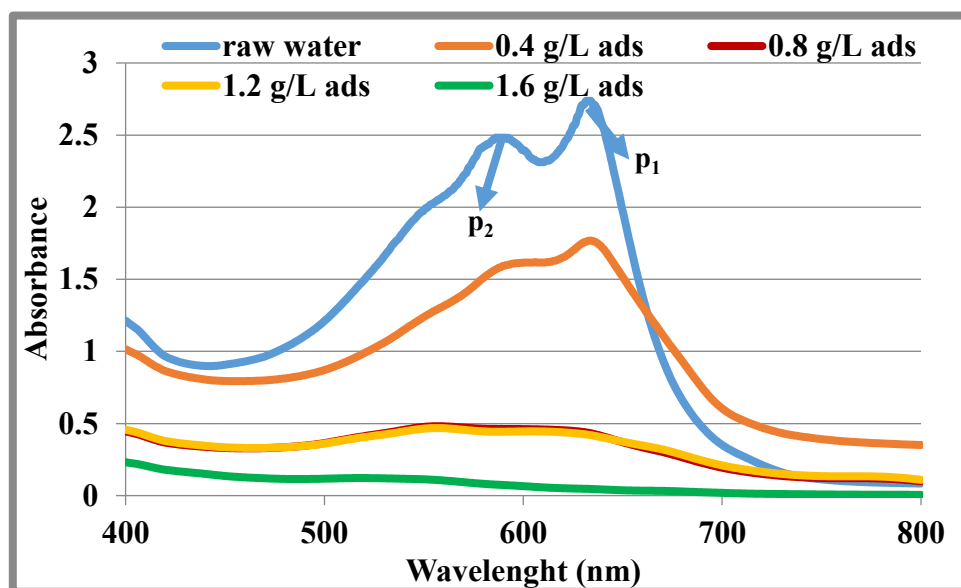


Figure 8. Treatment of real textile wastewater by adsorption (original wastewater pH = 4.62)

The removal increased as the adsorbent concentration increased from 0.4 to 1.6 g/L, increasing the surface area of the active sites responsible for color removal from wastewater. The absorbance values at the main points of peak 1 (p1; 632 nm) and peak 2 (p2; 589 nm) given by raw water decreased by 98.3% and 97.0%, respectively, at a 1.6 g/L adsorbent dosage in a 30 min contact time. These results showed that 100% Co-compound **3** complex can be used in the treatment of textile wastewater.

3.7. Effect of Contact Time and Adsorption Kinetics

The adsorption rate is determined via the contact time between the adsorbent and the adsorbate, and it plays an important role in determining the optimum adsorption time. When designing adsorbents for process optimization, contact time is also an issue that should be evaluated from an economic perspective [53]. For this purpose, samples were taken at the specified time intervals during the 60-min contact time under the optimized conditions for dyes, and the efficiency values were determined, and the effect of the contact time was tried to be revealed. A very fast step is observed in the first ten minutes in the adsorption process of BR dye. The large number of active sites and the rapid adsorption of BR dye onto the adsorbent surface can explain this situation. After this stage, the adsorption process slowed down due to the gradual occupation of these active sites on the adsorbent surface by adsorbent molecules. It was observed that equilibrium adsorption reached 92.23% removal efficiency within 50 min (Fig. 9). Different trends are observed during AR 337 dye adsorption. Quite high adsorption occurred within the first minute, then with slight increases, equilibrium was reached with 86.18% removal efficiency at 40 minutes. The adsorption capacity increased from 161.92 mg/g to 461.14 mg/g, from 616.85 to 861.8 mg/g, and from for BR and AB 337 respectively, when the contact time changes from 1 min to 50 min for sorbent mass 0.1 g/L.

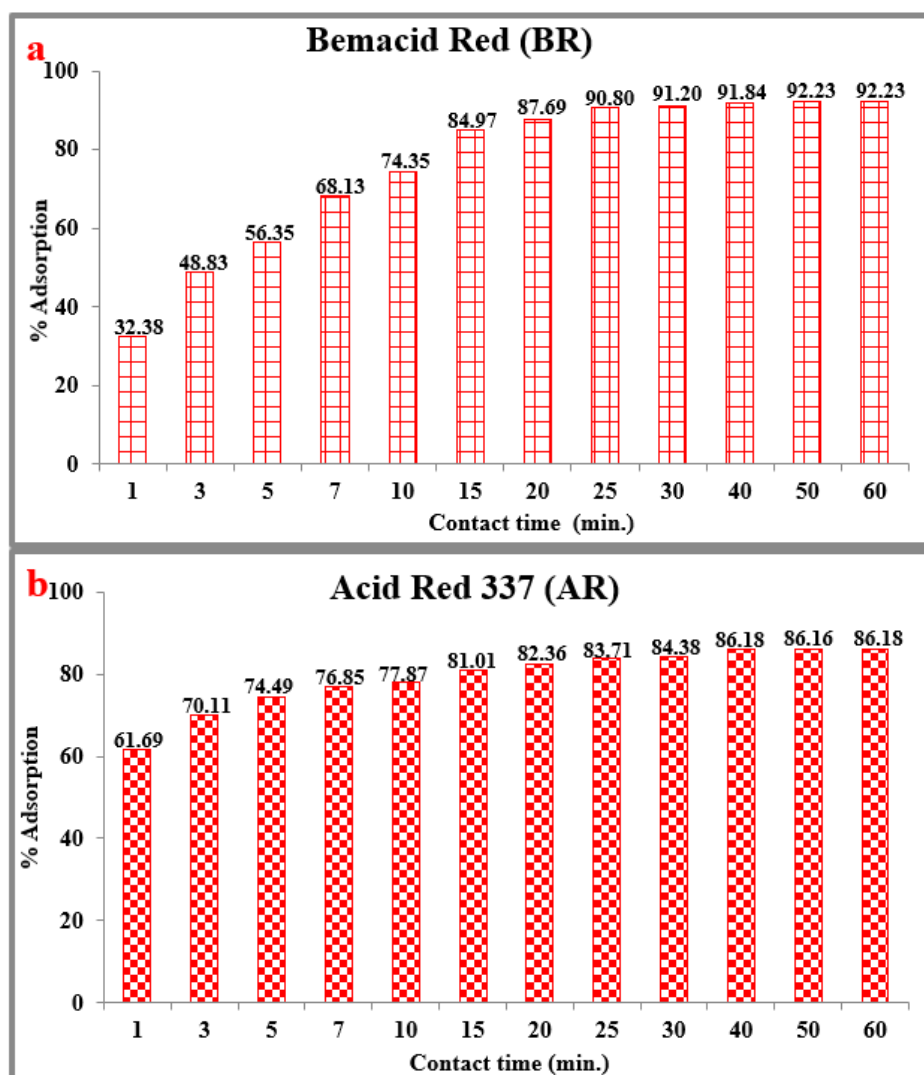


Figure 9. Effect of contact time on the adsorption process of **a)** bemacid red (BR), and **b)** Acid red 337.

Fitting experimental data with different kinetic models provides us with predictive information about adsorption rate, process model, and whether the interaction between adsorbent/adsorbate is physical or chemical [54]. Various kinetic models have been proposed to characterize the adsorption process, i.e., to determine what kind of mechanism plays a role during the adsorption of dye onto the adsorbent surface. In this study, Pseudo first order (Lagergren), Pseudo second order (Ho-McKay), Elovich, and Weber-Morris linear kinetic models were applied to investigate the removal adsorption process kinetics of BR and AR 337 by Co-compound **3** complex, and the results are given in Figure 10.

As the correlation coefficient values approach 1, the experimental kinetic data perfectly align with the kinetic model. The data obtained from these linear models are given in Table 1. When the R^2 values in Table 1 are examined, it is seen that the adsorption kinetics fits the Pseudo Second-order (Ho-McKay) model more for both dyes. Additionally, the equilibrium adsorption capacity (q_e) calculated using the Pseudo Second-order kinetic model was found to be closer to the equilibrium adsorption capacity obtained from experiments. However, there was a large deviation in the q_e values obtained in the other models. This result reveals that the decisive step of the adsorption process is chemisorption, and the adsorption mechanism is characterized by mass transfer to the adsorbent surface. In recent studies of other systems, the results of adsorption kinetics indicate that pseudo-second order accurately represents the experimental data in many instances. The pseudo-second-order kinetic model has been successfully

applied to explain the kinetics of Everzol yellow 3RS [55], removal of water from biodiesel by resin [56] and removal of Cu(II) ions [57] from aqueous media. In addition, since the value of $k_2 = 0.0011$ for AR 337 dye is greater than $k_2 = 0.0008$ for BR dye, the sorption rate of AR 337 dye was found to be higher than the sorption rate of BR dye.

According to the Weber and Morris model, as seen in Figure 10 d, the fact that the linear parts of the curves do not pass through the origin and that the C value is not 0 (indicating that the mentioned curve does not pass through the origin), as seen in Table 1, indicates that intraparticle diffusion is not a limiting component in the adsorption of dye molecules in the adsorbent. In other words, this suggests that the mechanism for the adsorption of BR and AR 337 dyes is more complicated.

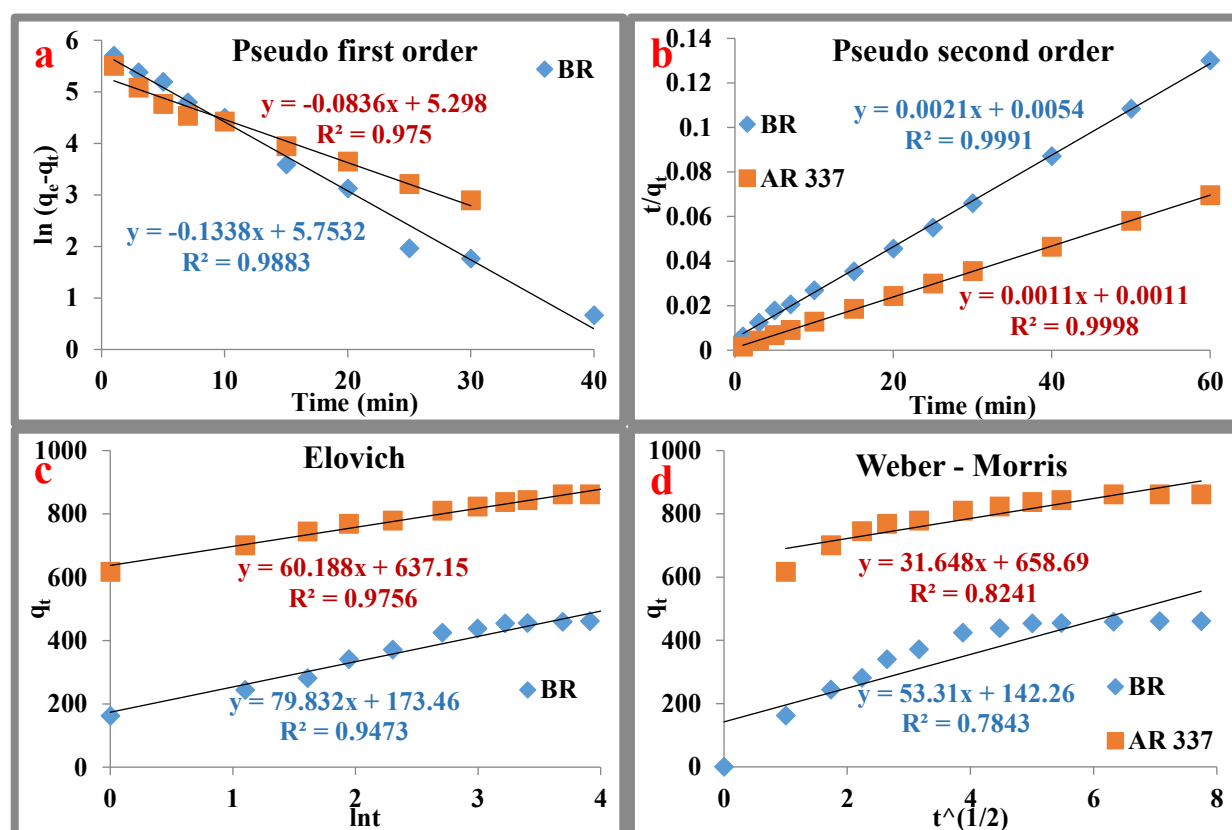


Figure 10. a) Pseudo first order kinetic model, b) Pseudo second order kinetic model, c) Elovich kinetic model, d) Weber-Morris kinetic model.

Table 1. Parameters and correlation coefficients of kinetic models

	Pseudo-first order				Pseudo-second order			Elovich			Weber-Morris		
	$q_e \text{ exp.}$	k_1	q_e	R^2	k_2	q_e	R^2	α	β	R^2	K_{id}	C	R^2
BR	461.2	-0.1338	315.2	0.9883	0.0008	476.2	0.9991	700.7	0.0125	0.9473	53.31	142.26	0.7843
AR 337	861.8	-0.0972	172.2	0.9605	0.0011	909.1	0.9998	2369886	0.0166	0.9756	69.48	460.36	0.51

3.8. Adsorption Isotherm

The relationship between the amount of adsorbed substance and the concentration of the substance remaining in the solution is described by adsorption isotherms. In the literature, many different isotherms, such as Langmuir, Freundlich, Temkin, and Dubinin-Radushkevich (D-R), are commonly used to gather information about how the system functions in adsorption processes. With the help of

these equations, the surface properties of the adsorbent and the relationship between the adsorbent and the adsorbate can be defined. In addition, the maximum adsorption capacity, adsorption density, and heat of adsorption can also be determined [54]. In this study, linear forms of the above equations were used to describe the equilibrium data.

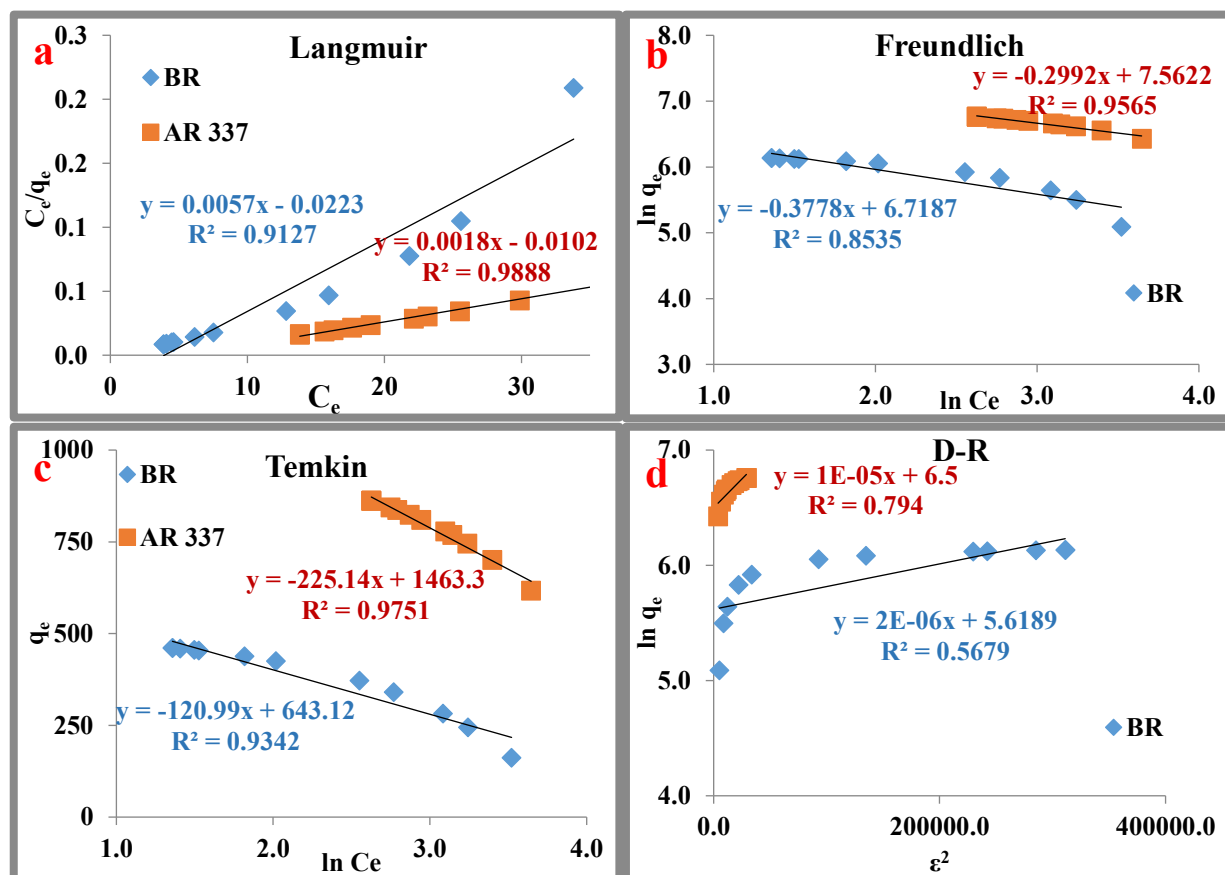


Figure 11. a) Langmuir, b) Freundlich, c) Temkin, and d) Dubinin-Radushkevich isotherm models.

To determine which isotherm, the adsorption process of BR and AR 337 dyes with Co/compound 3 complex fits, first, the R^2 values of the plotted graphs were examined. While high correlation coefficients ($R^2=0.9342$) were obtained by applying the experimental results to the Temkin adsorption isotherm model for BR, an approximate correlation coefficient ($R^2=0.9127$) was obtained with the Langmuir isotherm. Temkin constants K_T , which are the equilibrium binding constants, and the B constant related to the heat of adsorption are reported in Table 2. According to the Temkin isotherm, B values <20 J/mol are attributed to chemisorption dominated by physisorption. The maximum adsorption capacity (q_m) was obtained as 175.4 mg/g. The equilibrium parameter of the Langmuir isotherm is R_L : The R_L value determines whether the isotherm is unfavorable ($R_L>1$), linear ($R_L=1$), favorable ($0<R_L<1$), or irreversible ($R_L=0$) [58, 59]. Since the R_L value is calculated as 0.083, it indicates that the adsorbent used is suitable for BR adsorption.

When the AR 337 adsorption results were evaluated using the Langmuir adsorption isotherm, a high correlation coefficient ($R^2=0.9888$) was obtained, while lower correlation coefficients were observed in the Freundlich ($R^2=0.9565$) and Temkin models ($R^2=0.9751$). The maximum adsorption capacity (q_m) was determined to be 555.56 mg/g. In addition, the dimensionless number value of R_L was calculated as 0.067. Since these values are $0<R_L<1$, it shows that the adsorbent used was suitable for AR 337 adsorption. The $1/n$ value found from the Freundlich model was 0.299, indicating that there may be heterogeneous regions on the adsorbent surface and that the adsorption ability is good. High K_F value (1924.1) indicates that the adsorbent has a high adsorption capacity. The E value in the D-R isotherm was

found to be 0.224 kJ/mol, and since it is less than 8 kJ/mol, the adsorption process is considered physical. However, the R^2 value of the D-R isotherm, being 0.794, suggests that the adsorption process fits the D-R isotherm less well than other isotherms.

The isotherm correlation coefficients (R^2 values) illustrated in Figure 11 were used to evaluate their applicability, and the R^2 values obtained for each isotherm are given in Table 2. In addition, the constants for each isotherm were determined by using the slopes and shifts of the graphs in Figure 11, and these constants are also given in Table 2.

3.9. Thermodynamic Analyses

Thermodynamic analyses were performed at four different temperatures: 20, 30, 40, and 50 °C (Fig. 12). As shown in Table 3, the negative enthalpy change for AR 337 adsorption indicates that the process is exothermic, and operating at lower temperatures can enhance the adsorption efficiency. The positive enthalpy change observed in BR adsorption indicates that the process is endothermic, and conducting the adsorption at higher temperatures may result in greater efficiency. While the negative Gibbs free energy change (ΔG°) for both dyes indicates a spontaneous adsorption, the absolute values greater than 20 kJ/mol suggest that the process is physical adsorption [60]. However, the fact that ΔH° values are also small, <80 kJ/mol, supports that the process is physical. The positive changes in entropy suggest that the disorder at the adsorbent-adsorbate interface has slightly increased.

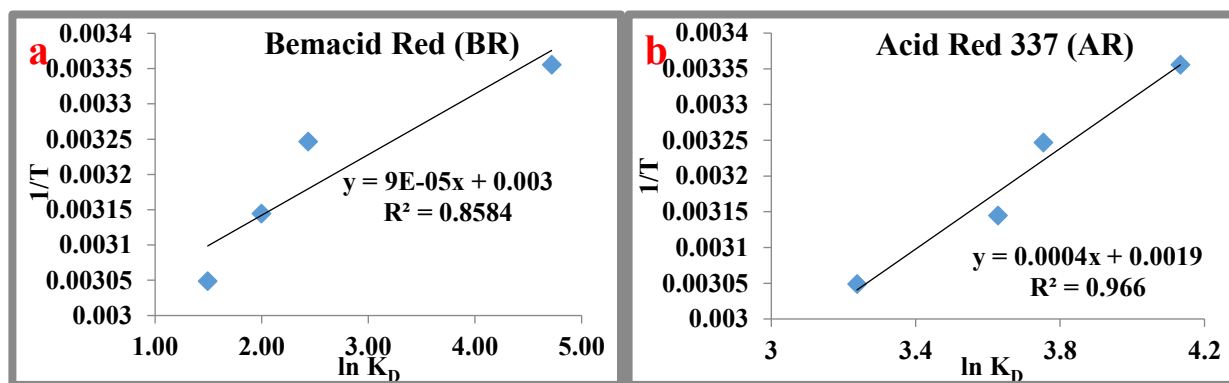


Figure 12. Thermodynamic model

4. CONCLUSIONS

In this study, the adsorption mechanism of BR and AR 337 dyes on the synthesized Co or Ni 2-(naphthalen-1-yloxy) acetohydrazide adsorbents (Co or Ni compound **3** complexes) was investigated by the batch adsorption technique, and it was found that Co/compound **3** complex can be used as a potential adsorbent in dye removal. As a result of the experimental data, the optimum adsorption conditions for BR and AR 337 are as follows: at the original sample pH (6.7), 0.1 g/L adsorbent dosage, 50 mg/L BR and 100 mg/L AR 337 initial pollutant concentration, 40 min contact time, 91.84% BR and 96.18% AR 337 removal was achieved. Under these conditions, the maximum adsorption capacities were calculated as 461.14 mg/g for BR and 861.8 mg/g for AR 337.

The adsorption of BR and AR 337 with Co/compound **3** complex was found to be compatible with pseudo-second-order kinetics in terms of kinetics. The equilibrium adsorption capacity calculated in the kinetic model was found to be closer to the equilibrium adsorption capacity obtained from the experiments. Furthermore, it was observed that the kinetic adsorption process took place through chemical adsorption and mass transfer to the surface of the adsorbent. Additionally, when the obtained rate constants were examined, the adsorption rate of AR 337 dye was higher than that of BR dye. The adsorption of BR and AR 337 by Co/compound **3** complex was found to be compatible with Temkin and

Langmuir isotherms, respectively, in terms of isotherms. According to the Temkin isotherm, it was shown that the mechanism of BR occurred as the chemisorption of the adsorbate on the sorbent. The experimental results for AR 337 fit the Langmuir adsorption isotherm model, the maximum adsorption capacity is 555.56 mg/g, and the R_L value shows that the adsorbent used is suitable for AR 337 adsorption.

Table 2. Constants for isotherm models

Isotherm model	pollutant	Parametre	Value
Langmuir	BR	K_L	-0.26
		q_{max}	175.4
		R^2	0.9127
	AR 337	K_L	-0.176
		q_{max}	555.56
		R^2	0.9888
Freundlich	BR	K_F	827.7
		n	2.65
		R^2	0.8535
	AR 337	K_F	1924.1
		n	3.34
		R^2	0.9565
Temkin	BR	K_T	0.00489
		B	-20.48
		R^2	0.9342
	AR 337	K_T	0.0015
		B	-11
		R^2	0.9751
D-R	BR	K_{D-R}	2×10^{-6}
		E	0.5
		q_{max}	275.6
		R^2	0.5679
	AR 337	K_{D-R}	10^{-5}
		E	0.224
		q_{max}	665.1
		R^2	0.794

Table 3. Constants of the thermodynamic model

	ΔH° (kJ/mol)	ΔS° (J/mol/K)	ΔG° (kJ/mol)			
			298 K	308 K	318 K	328 K
BR	41.57	0.025	-11689.3	-6234.76	-5277.69	-4071.67
AR 337	-0.00333	0.016	-10239.6	-9610.98	-9590.6	-8827.68

Thermodynamic analyses show that adsorption of AR 337 dye is exothermic and low temperatures favor adsorption; for BR, the mechanism is endothermic and high temperatures favor adsorption. However, ΔH° values are less than <80 kJ/mol, indicating that the processes are physical. The fact that the

standard free energy change values are negative for both dyes indicates that the adsorption occurs spontaneously. In addition, the absolute values of ΔG° are greater than 20 kJ/mol, supporting that the adsorption process is physical adsorption. The data obtained in the study determined that the adsorbents used to remove pollutants such as paint from aqueous environments exhibited good performance.

Declaration of Ethical Standards

The authors declare that they comply with all ethical standards.

Credit Authorship Contribution Statement

The authors contributed equally to the study's conception and design.

Mehmet Türkyılmaz: Conceptualization, Formal analysis, Investigation, Methodology, Resources, Writing – original draft, Visualization,

Farabi Temel: Methodology, Investigation, Validation, Visualization, Writing – review & editing,

Declaration of Competing Interest

The authors have no competing interests to declare that are relevant to the content of this article.

Funding / Acknowledgements

This research did not receive any specific grant from funding agencies in the public, commercial, or not-for-profit sectors.

Data Availability

All data generated or analyzed during this study are included in this published article.

5. REFERENCES

- [1] F. Cengel and F. Temel, "Removal of p-nitrophenol from aqueous solutions by calixarene based graphene oxide" *Konya Journal of Engineering Sciences*, 9, 79-90, 2021.
- [2] T. Uzun, İ. Yılmaz, A. I. Vaizogullari, and M. Ugurlu, "Çeşitli Adsorbentler Kullanılarak Flumequin'in (Antibiyotik türü) Atık Sulardan Adsorbsiyon Yöntemiyle Giderilmesi", *Akademik Platform, ISEM2014 Adıyaman*, pp. 1411-1420, 2014.
- [3] L. Meili *et al.*, "Adsorption of methylene blue on agroindustrial wastes: experimental investigation and phenomenological modelling," *Progress in biophysics and molecular biology*, vol. 141, pp. 60-71, 2019.
- [4] F. Kooli *et al.*, "Waste bricks applied as removal agent of basic blue 41 from aqueous solutions: base treatment and their regeneration efficiency," *Applied Sciences*, vol. 9, no. 6, p. 1237, 2019.
- [5] B. Hatimi *et al.*, "Physicochemical and statistical modeling of reactive Yellow 145 enhanced adsorption onto pyrrhotite Ash-Based novel (Catechin-PG-Fe)-Complex," *Materials Science for Energy Technologies*, vol. 6, pp. 65-76, 2023.
- [6] S. Sarkar, A. Banerjee, U. Halder, R. Biswas, and R. Bandopadhyay, "Degradation of synthetic azo dyes of textile industry: a sustainable approach using microbial enzymes," *Water Conservation Science and Engineering*, vol. 2, pp. 121-131, 2017.
- [7] Y. Liu *et al.*, "Quantitative structure-activity relationship (QSAR) guides the development of dye removal by coagulation," *Journal of Hazardous Materials*, vol. 438, p. 129448, 2022.
- [8] I. Levchuk, J. J. R. Márquez, and M. Sillanpää, "Removal of natural organic matter (NOM) from water by ion exchange—a review," *Chemosphere*, vol. 192, pp. 90-104, 2018.

- [9] F. Temel, M. Turkyilmaz, and S. Kucukcongar, "Removal of methylene blue from aqueous solutions by silica gel supported calix[4]arene cage: Investigation of adsorption properties," *European Polymer Journal*, vol. 125, p. 109540, 2020.
- [10] C. Balcik-Canbolat, T. Olmez-Hanci, C. Sengezer, H. Sakar, A. Karagunduz, and B. Keskinler, "A combined treatment approach for dye and sulfate-rich textile nanofiltration membrane concentrate," *Journal of Water Process Engineering*, vol. 32, p. 100919, 2019.
- [11] A. G. J. Alwindawi, M. Turkyilmaz, and S. Kucukcongar, "Synthesis of magnetic photocatalyst by photochemical deposition and co-precipitation techniques: investigation of its photocatalytic and sonophotocatalytic activity for dye removal," *International Journal of Environmental Analytical Chemistry*, vol. 102, no. 19, pp. 8419-8433, 2022.
- [12] M. Türkyilmaz, "A comparative study of free chlorine activated by Fe²⁺ and UV C light catalysts in the treatment of real and simulated textile wastewater: Optimization, reactive species and phytotoxicity assessment," *Journal of Water Process Engineering*, vol. 49, p. 103161, 2022.
- [13] M. Jonstrup, N. Kumar, M. Murto, and B. Mattiasson, "Sequential anaerobic-aerobic treatment of azo dyes: decolourisation and amine degradability," *Desalination*, vol. 280, no. 1-3, pp. 339-346, 2011.
- [14] A. Kuleyin, A. Gök, and F. Akbal, "Treatment of textile industry wastewater by electro-Fenton process using graphite electrodes in batch and continuous mode," *Journal of Environmental Chemical Engineering*, vol. 9, no. 1, p. 104782, 2021.
- [15] M. Ghanei, A. Rashidi, H.-A. Tayebi, and M. E. Yazdanshenas, "Removal of acid blue 25 from aqueous media by magnetic-SBA-15/CPAA super adsorbent: adsorption isotherm, kinetic, and thermodynamic studies," *Journal of Chemical & Engineering Data*, vol. 63, no. 9, pp. 3592-3605, 2018.
- [16] E. I. Unuabonah and A. Taubert, "Clay-polymer nanocomposites (CPNs): Adsorbents of the future for water treatment," *Applied clay science*, vol. 99, pp. 83-92, 2014.
- [17] M. T. Yagub, T. K. Sen, S. Afroze, and H. M. Ang, "Dye and its removal from aqueous solution by adsorption: a review," *Advances in Colloid and Interface Science*, vol. 209, pp. 172-184, 2014.
- [18] B. Abbou *et al.*, "Improved removal of methyl orange dye by adsorption using modified clay: combined experimental study using surface response methodology," *Inorganic Chemistry Communications*, vol. 155, p. 111127, 2023.
- [19] S. Mallakpour, F. Sirous, and M. Dinari, "Comparative study for removal of cationic and anionic dyes using alginate-based hydrogels filled with citric acid-sawdust/UiO-66-NH₂ hybrid," *International Journal of Biological Macromolecules*, vol. 238, p. 124034, 2023.
- [20] X. Qu, P. J. Alvarez, and Q. Li, "Applications of nanotechnology in water and wastewater treatment," *Water Research*, vol. 47, no. 12, pp. 3931-3946, 2013.
- [21] D. Y. Kola and S. Edebalı, "Exploring Mil-53 (Al) Adsorption Efficiency For Indigo Carmine Dye" *Konya Journal of Engineering Sciences*, 12, 419-431, 2024.
- [22] W. M. Singh and J. B. Baruah, "Coordination polymers of cadmium with (4-carbomethoxy-naphthalen-1-yl)oxy) acetic acid derivatives," *Polyhedron*, vol. 29, no. 6, pp. 1543-1550, 2010.
- [23] N. Boukabcha *et al.*, "Synthesis, crystal structure, spectroscopic characterization and nonlinear optical properties of (Z)-N'-(2,4-dinitrobenzylidene)-2-(quinolin-8-yl)oxy) acetohydrazide," *Journal of Molecular Structure*, vol. 1194, pp. 112-123, 2019/10/15/ 2019.
- [24] D. Kılınç and Ö. Şahin, "Synthesis of polymer supported Ni (II)-Schiff Base complex and its usage as a catalyst in sodium borohydride hydrolysis," *International Journal of Hydrogen Energy*, vol. 43, no. 23, pp. 10717-10727, 2018/06/07/ 2018.
- [25] S. Lagergren, "Zur Theorie der sogenannten Adsorption gelöster Stoffe. Bil. K. Svenska Venteskapsakad, Handl. 24 (1898) as cited by Wasay et al," *Water Res*, vol. 30, pp. 1143-1148, 1996.
- [26] Y. S. Ho and G. McKay, "The kinetics of sorption of divalent metal ions onto sphagnum moss peat," *Water Research*, vol. 34, no. 3, pp. 735-742, 2000.
- [27] S. Y. Elovich and O. Larinov, "Theory of adsorption from solutions of non electrolytes on solid (I) equation adsorption from solutions and the analysis of its simplest form,(II) verification of the

- equation of adsorption isotherm from solutions," *Izv. Akad. Nauk. SSSR, Otd. Khim. Nauk*, vol. 2, no. 2, pp. 209-216, 1962.
- [28] W. J. Weber Jr and J. C. Morris, "Kinetics of adsorption on carbon from solution," *Journal of the sanitary engineering division*, vol. 89, no. 2, pp. 31-59, 1963.
- [29] I. Langmuir, "The adsorption of gases on plane surfaces of glass, mica and platinum," *Journal of the American Chemical Society*, vol. 40, no. 9, pp. 1361-1403, 1918.
- [30] H. Freundlich, "Colloid and capillary chemistry, EP Dutton and Co," *New York*, pp. 132-137, 1928.
- [31] M. J. Temkin and V. Pyzhev, "Recent modifications to Langmuir isotherms," 1940.
- [32] M. Dubinin, "The equation of the characteristic curve of activated charcoal," in *Dokl. Akad. Nauk. SSSR.*, 1947, vol. 55, pp. 327-329.
- [33] B. Ali Fil, M. Korkmaz, and G. Özmetin, "An empirical model for adsorption thermodynamics of copper (II) from solutions onto illite clay-batch process design," *Journal of the Chilean Chemical Society*, vol. 59, no. 4, pp. 2686-2691, 2014.
- [34] E. C. Lima, A. Hosseini-Bandegharai, J. C. Moreno-Piraján, and I. Anastopoulos, "A critical review of the estimation of the thermodynamic parameters on adsorption equilibria. Wrong use of equilibrium constant in the Van't Hoof equation for calculation of thermodynamic parameters of adsorption," *Journal of molecular liquids*, vol. 273, pp. 425-434, 2019.
- [35] S. S. Al-Muhanaa and A. H. Al-Khafagy, "Preparation and Biological Activities of New Heterocyclic Azo Ligand and Some of Its Chelate Complexes," *Nano Biomedicine and Engineering*, vol. 10, no. 1, pp. 46-55, 2018.
- [36] M. G. Radhika *et al.*, "Electrochemical studies on Ni, Co & Ni/Co-MOFs for high-performance hybrid supercapacitors," *Materials Research Express*, vol. 7, no. 5, p. 054003, 2020/05/11 2020.
- [37] A. V. Buntić, M. D. Pavlović, D. G. Antonović, S. S. Šiler-Marinković, and S. I. Dimitrijević-Branković, "A treatment of wastewater containing basic dyes by the use of new strain *Streptomyces microflavus* CKS6," *Journal of Cleaner Production*, vol. 148, pp. 347-354, 2017.
- [38] N. Douara, M. Benzekri Benallou, M. Termoul, Z. Mekibes, B. Bestani, and N. Benderdouche, "Removal of textile dyes on a biosorbent based on the leaves of *Atriplex halimus*," *Iranian Journal of Chemistry and Chemical Engineering*, vol. 41, no. 11, pp. 3726-3741, 2022.
- [39] B. Maimoun, A. Djafer, L. Djafer, R.-M. Marin-Ayral, and A. Ayral, "Wastewater treatment using a hybrid process coupling adsorption on marl and microfiltration," *Membrane Water Treatment*, 2020.
- [40] A. Yıldız, "Adsorption of Acid Red 114 onto Fe₃O₄@ Caffeic acid recyclable magnetic nanocomposite," *Journal of the Turkish Chemical Society Section A: Chemistry*, vol. 4, no. 1, pp. 327-340, 2017.
- [41] S.-W. Nam, D.-J. Choi, S.-K. Kim, N. Her, and K.-D. Zoh, "Adsorption characteristics of selected hydrophilic and hydrophobic micropollutants in water using activated carbon," *Journal of hazardous materials*, vol. 270, pp. 144-152, 2014.
- [42] R. Boudia, G. Mimanne, K. Benhabib, and L. Pirault-Roy, "Preparation of mesoporous activated carbon from date stones for the adsorption of Bemacid Red," *Water Science and Technology*, vol. 79, no. 7, pp. 1357-1366, 2019.
- [43] M. Kılıç and A. S. K. Janabi, "Investigation of dyes adsorption with activated carbon obtained from *Cordia myxa*," *Bilge International Journal of Science and Technology Research*, vol. 1, no. 2, pp. 87-104, 2017.
- [44] D. Raca, L. Vukić, D. Drljaca, and D. Dragić, "Adsorption of Bemacid Red Dye from Aqueous Solutions on Coal Fly Ash Modified with Hydrochloric Acid," *Journal of Chemists, Technologists and Environmentalists*, vol. 4, no. 1, pp. 30-39, 2023.
- [45] S. Feddane, K. Oukebdane, M. A. Didi, A. Didi, A. Amara, and O. Larabi, "Removal of textile dye Bemacid Red from water using *Casuarina equisetifolia* needles: kinetic and thermodynamic modeling," *Desalination and Water Treatment*, vol. 289, pp. 248-257, 2023.

- [46] A. Özer, G. Akkaya, and M. Turabik, "The biosorption of Acid Red 337 and Acid Blue 324 on *Enteromorpha prolifera*: the application of nonlinear regression analysis to dye biosorption," *Chemical Engineering Journal*, vol. 112, no. 1-3, pp. 181-190, 2005.
- [47] I. Slatni *et al.*, "Mesoporous silica synthesized from natural local kaolin as an effective adsorbent for removing of Acid Red 337 and its application in the treatment of real industrial textile effluent," *Environmental Science and Pollution Research*, vol. 27, pp. 38422-38433, 2020.
- [48] S. Shrestha, G. Son, S. H. Lee, and T. G. Lee, "Isotherm and thermodynamic studies of Zn (II) adsorption on lignite and coconut shell-based activated carbon fiber," *Chemosphere*, vol. 92, no. 8, pp. 1053-1061, 2013.
- [49] H. Cherifi, B. Fatiha, and H. Salah, "Kinetic studies on the adsorption of methylene blue onto vegetal fiber activated carbons," *Applied Surface Science*, vol. 282, pp. 52-59, 2013/10/01/ 2013.
- [50] S. Banerjee, G. C. Sharma, M. Chattopadhyaya, and Y. C. Sharma, "Kinetic and equilibrium modeling for the adsorptive removal of methylene blue from aqueous solutions on of activated fly ash (AFSH)," *Journal of Environmental Chemical Engineering*, vol. 2, no. 3, pp. 1870-1880, 2014.
- [51] Y.-S. Ho and A. E. Ofomaja, "Pseudo-second-order model for lead ion sorption from aqueous solutions onto palm kernel fiber," *Journal of Hazardous Materials*, vol. 129, no. 1-3, pp. 137-142, 2006.
- [52] A. Djafer, L. Djafer, B. Maimoun, A. Iddou, S. Kouadri Mostefai, and A. Ayrat, "Reuse of waste activated sludge for textile dyeing wastewater treatment by biosorption: performance optimization and comparison," *Water and Environment Journal*, vol. 31, no. 1, pp. 105-112, 2017.
- [53] M. Sciban, T. Vulic, D. Kukic, J. Prodanovic, and M. Klasnja, "Characterization of raw and treated sugar beet shreds for copper ions adsorption," *Desalination and Water Treatment*, vol. 57, no. 31, pp. 14590-14597, 2016.
- [54] T. M. Elmorsi, Z. H. Mohamed, W. Shopak, and A. M. Ismaiel, "Kinetic and equilibrium isotherms studies of adsorption of Pb (II) from water onto natural adsorbent," *Journal of Environmental Protection*, vol. 5, no. 17, pp. 1667-1681, 2014.
- [55] M. Behnajady, N. Modirshahla, and F. Ghanbary, "A kinetic model for the decolorization of CI Acid Yellow 23 by Fenton process," *Journal of Hazardous Materials*, vol. 148, no. 1-2, pp. 98-102, 2007.
- [56] Z. Ç. Okumuş and T. H. Doğan, "Biyodizeldeki suyun reçine ile uzaklaştırılması: adsorpsiyon izotermi, kinetiği ve termodinamik incelemesi," *Avrupa Bilim ve Teknoloji Dergisi*, no. 15, pp. 561-570, 2019.
- [57] S. Tunç, T. Gürkan, and O. Duman, "On-line spectrophotometric method for the determination of optimum operation parameters on the decolorization of Acid Red 66 and Direct Blue 71 from aqueous solution by Fenton process," *Chemical Engineering Journal*, vol. 181, pp. 431-442, 2012.
- [58] C. H. Chan, C. H. Chia, S. Zakaria, M. S. Sajab, and S. X. Chin, "Cellulose nanofibrils: a rapid adsorbent for the removal of methylene blue," *RSC Advances*, vol. 5, no. 24, pp. 18204-18212, 2015.
- [59] E. Özçelik, F. Temel, and M. Tabakci, "Sensing of p-nitrophenol in aqueous media on QCM sensor coated with calixarene derivative immobilized merrifield resin", *Konya Journal of Engineering Sciences* 7, 594-603, 2019.
- [60] R. Li, N. Liang, X. Ma, B. Chen, and F. Huang, "Study on the adsorption behavior of glycerin from fatty acid methyl esters by a tertiary amine-type anion exchange resin," *Journal of Chromatography A*, vol. 1586, pp. 62-71, 2019.